



A NOVEL INDOOR VISIBLE LIGHT COMMUNICATION SYSTEM USING MIMO TECHNIQUES AND LED PLACEMENT FOR ENHANCED SIGNAL QUALITY

Faheem Mollick

Shanti Rathore

Kiran Tigga

India.

ABSTRACT

This paper presents a novel approach to enhancing the performance of indoor Visible Light Communication (VLC) systems by integrating Multiple-Input Multiple-Output (MIMO) techniques and a arrangement of Light Emitting Diodes (LEDs). With the increasing demand for high-speed wireless communication, VLC offers a promising solution, leveraging the unlicensed visible light spectrum. In this work, we investigate the potential of MIMO for improving data throughput, signal-to-noise ratio (SNR), and overall system efficiency in VLC systems. The proposed system utilizes a 3D LED configuration, which optimizes coverage and illuminance within indoor environments. Simulation results demonstrate the effectiveness of the proposed system in enhancing data rates and reliability, particularly when compared to traditional Single Input Single Output (SISO) systems. Furthermore, the paper explores the impact of different

parameters, such as the use of optical lenses and varying LED distances, on the performance of the system. The findings highlight the significant improvements in system performance, making the proposed VLC architecture a strong candidate for future indoor communication applications.

Keywords: LED, MIMO, MISO, SISO, SNR, VLC.

Cite this Article: Faheem Mollick, Shanti Rathore, Kiran Tigga. A Novel Indoor Visible Light Communication System Using MIMO Techniques and LED Placement for Enhanced Signal Quality. *International Journal of Electronics and Communication Engineering and Technology (IJECEET)*, 16(1), 2025, pp. 1-20.

https://iaeme.com/MasterAdmin/Journal_uploads/IJECEET/VOLUME_16_ISSUE_1/IJECEET_16_01_001.pdf

1. INTRODUCTION

The rapid evolution of wireless communication technologies is a key driver in meeting the requirements of the fifth generation (5G) and beyond (B5G) networks, which demand faster data speeds, ultra-low latency, and massive connectivity [1]. Among the core objectives of 5G is to enhance mobile throughput, reduce communication delays, and accommodate the increasing number of connected devices [2]. However, these advancements are hindered by the limited availability of radio frequency (RF) spectrum, which has become increasingly congested and regulated, impacting the performance of existing communication technologies like Wi-Fi, Bluetooth, and ZigBee.

Indoor wireless communication, particularly within home and industrial environments, generates the majority of global data traffic [3], making it an area of growing concern. The demand for internet connectivity is expected to surge as the global population becomes more connected, with projections indicating that two-thirds of the world's population will be internet users by the next decade [4]. Consequently, there is an urgent need for new communication technologies and wider bandwidth to improve user experience and ensure reliable connectivity.

Visible Light Communication (VLC) has emerged as a promising solution to address these challenges. VLC utilizes visible light signals to transmit data, providing a unique opportunity to repurpose existing lighting infrastructure for high-speed wireless communication. The visible light spectrum, spanning from 380 nm to 780 nm, offers an

expansive bandwidth of nearly 400 THz [5], which is largely untapped compared to RF communication bands. This spectrum provides an excellent alternative for enhancing communication networks, especially given the constraints of the RF spectrum and the growing demands for IoT connectivity [6].

VLC systems offer several advantages over traditional RF communication, such as the availability of unlicensed spectrum, immunity to RF interference, and enhanced security, as light cannot penetrate walls. VLC systems are also cost-effective, utilizing existing lighting infrastructure without the need for additional equipment, while offering low-cost transmitters and receivers that are commercially available. Furthermore, VLC technology eliminates the risk of electromagnetic interference, which is critical in sensitive environments like hospitals and airplanes.

With the growing adoption of Light Emitting Diodes (LEDs), which are increasingly replacing traditional lighting systems due to their longer lifespan and higher efficiency [7] [8], VLC is poised to become a significant component of future communication networks. The potential integration of VLC into next-generation cellular networks, as well as its applicability in diverse environments such as underwater, satellite, and vehicle-to-vehicle communications, further underscores its importance.

In order to realize the full potential of VLC, it is essential to explore new transmission techniques. One such approach is Multiple-Input Multiple-Output (MIMO) technology, which has been successfully applied in RF communication to enhance data throughput and system reliability. MIMO systems use multiple transmitters and receivers to create parallel communication channels, thereby increasing capacity without requiring additional power or bandwidth. In the context of VLC, MIMO has the potential to significantly improve spectral efficiency and communication performance, making it an essential area of research for the future of wireless optical communication.

This paper proposes a novel indoor VLC system based on a 3D arrangement of LEDs and investigates the application of MIMO techniques to enhance data throughput and system efficiency. The goal is to optimize VLC performance in indoor environments by improving key parameters such as illuminance, received power, signal-to-noise ratio (SNR), and throughput, while minimizing the need for additional LEDs or power.

2. LITERATURE REVIEW

The potential of Visible Light Communication (VLC) as an alternative to traditional radio frequency (RF) systems has been explored in various studies. Early work by the authors of [9] and [10] proposed a versatile ultraviolet light communication (UVLC) channel model, incorporating the effects of absorption and scattering in underwater environments. These studies utilized statistical techniques to analyze the performance of UVLC systems, particularly in challenging scenarios involving different water types, transmitter/receiver configurations, and connection lengths. However, these models did not consider the impacts of channel coding, which is an essential component in modern communication systems.

The authors of [11] provided a mathematical model for UVLC systems under underwater conditions, incorporating key factors such as attenuation, scattering, and absorption. They focused on the effects of refractive index gradients on light signal propagation, using parameters like link distance, SNR, and bit error rate (BER) to assess system performance. The authors of [12] studied Line-of-Sight (LoS) LED-based Underwater Wireless Optical Communication (UWOC) systems and evaluated their performance using BER and SNR metrics. However, they did not investigate Non-Line-of-Sight (NLoS) propagation effects, which can significantly affect communication quality in practical scenarios.

Modulation techniques play a vital role in enhancing VLC system performance, particularly in environments with high ambient light. The authors of [13] introduced novel modulation schemes, including Carrierless Amplitude/Phase (CAP), Discrete Fourier Transform Spread-Orthogonal Frequency Division Multiplexing (DFT-S OFDM), and conventional OFDM. These schemes aimed to optimize system performance through digital signal processing techniques such as pre- and post-equalization, as well as nonlinear correction.

The authors of [14] compared modulation techniques such as Phase Shift Keying (PSK), Non-Return-to-Zero On-Off Keying (NRZ-OOK), and OFDM for VLC systems operating in environments with high ambient light. Their simulations indicated that PSK was the most effective modulation scheme for systems using rolling-shutter sensors.

Further studies have focused on underwater optical wireless communication, the authors of [14] examining a system with randomly located receivers and studying the effects of beam spread and scintillation on link distance and BER. The authors of [16] investigated vertical UVLC channels using a layered model and presented closed-form expressions for BER performance, which were validated through numerical simulations.

In terms of error-control coding, the authors of [17] proposed a channel coding scheme combining Forward Error Correction (FEC) codes with adaptive modulation to improve data rates and error correction in VLC systems under varying dimming conditions. Their results demonstrated significantly better performance compared to traditional coding methods, providing a foundation for future research in error control for UVLC and similar systems.

In the context of MIMO for optical wireless communication (OWC), several approaches have been explored. MIMO has been applied to optical systems to enhance capacity and reliability, particularly in RF communications [18] [19]. Spatial diversity (SD), spatial multiplexing (SMP), and spatial modulation (SM) are common MIMO techniques that offer significant improvements in communication systems by exploiting multiple degrees of freedom. In VLC, these techniques allow for the creation of parallel communication channels, leading to higher spectral efficiency and system capacity without additional power or bandwidth.

Despite the extensive work on VLC and MIMO systems, challenges remain in optimizing the efficiency and throughput of indoor VLC systems. This research aims to address these challenges by proposing a novel 3D LED arrangement and investigating the impact of MIMO techniques on VLC system performance. The combination of these innovations is expected to enhance the data rate and overall communication quality in indoor environments, paving the way for the integration of VLC into next-generation wireless networks.

3. PROPOSED METHODOLOGY

The main objective of communication systems is to achieve high throughput with high reliability. The transmission rate is related to the channel capacity, representing the maximum number of data transmitted at any time. The reliability of the transmission is related to the probability of error, inversely proportional to the signal-to-noise ratio. To improve both throughput and reliability, a simple solution is to increase the transmission power. However, in a multi-user environment, this also leads to an increase in interference. A second solution is to change the data modulation type, but this requires widening the transmission spectrum. The most recent technique is to use multiple antenna transmission and reception techniques, which improves both reliability and transmission rate while maintaining the same spectrum and transmission power. These systems are widely known as "multiple-input multiple-output" (MIMO) systems.

Various systems are used in this research for wireless transmission, such as:

3.1 SISO System

SISO (Single Input Single Output) system is a communication system introduced in the early days of wireless communication technology. It is the least complex and simplest wireless communication system compared to other systems. SISO system has only one antenna on both the transmitter and receiver side. Due to the presence of a single antenna on both sides, it is easy to use and implement, and it is cheaper because it does not require any additional processing on the transmitter and receiver side. SISO systems are now used in Wi-Fi, TV, and broadcasting communication technologies.

The channel capacity in a SISO system is represented by:

$$C = B \cdot \log_2 \left(1 + \frac{p}{N_0 B} \right) \quad (1)$$

Where:

- B : the bandwidth in Hz,
- P : the power of the useful signal expressed in Watt
- N_0 : the power spectral density of the noise in W/Hz,

After normalizing the capacity by the useful band B , we find:

$$C = \log_2(1 + \rho) \quad (2)$$

Where, ρ is the signal/noise ratio.

3.2 SIMO System

In a data transmission scheme, the SIMO system contains a single antenna on the transmitter side and multiple antennas on the receiver side, to combat channel fading. This system is also known as receive diversity. The received signal is combined and the overall signal-to-noise ratio is equal to the sum of the signal-to-noise ratios of each receiving antenna.

The channel capacity in a SIMO system is represented by:

$$C = B \cdot \log_2 \left(1 + N_r^2 \frac{p}{N_0 B} \right) \quad (3)$$

Where, N_r is the number of receiving antennas used at the receiver. And after normalization, we get:

$$C = B \cdot \log_2(1 + N_r^2 \rho) \quad (4)$$

3.3 MISO System

This is a spatial diversity technique in transmission where several antennas transmit signals, which are picked up by a single antenna in reception.

In this transmission mode, the signals emitted simultaneously by the N_t transmitting antennas are superimposed and received. Each antenna transmits the same symbol with an energy ES/N_t . In other words, the transmitted power is distributed between the number of antennas, so that:

$$P = \sum_{i=1}^{N_t} P_i \quad (5)$$

Where P_i is the power transmitted by each antenna. If the power is the same on all antennas, then we say that:

$$P = N_t \cdot P_i \quad (6)$$

The channel capacity in a MISO system is given by the following formula:

$$C = B \cdot \log_2 \left(1 + N_t \frac{P_i}{N_0 B} \right) = B \cdot \log_2 \left(1 + \frac{p}{N_0 B} \right) \quad (7)$$

After normalizing the capacity by the useful band B, we obtain:

$$C = \log_2(1 + \rho) \quad (8)$$

Equations (1) and (7) are identical, but in case of multiple paths, the MISO technique is more advantageous than the SISO technique because the probability of fading in N_t antennas is lower than in a single antenna.

3.4 MIMO System

MIMO technology offers the possibility to increase the throughput linearly with the number of receiving antennas, while counteracting the effects of channel fading. Therefore, it reduces the probability of fading and signal attenuation.

The difference between a MIMO (Multiple Input Multiple Output) system and a MISO (Multiple Input Single Output) system is that MIMO sends different packets to transmitting antennas operating at the same frequency, while MISO sends the same packets to transmitting antennas operating at the same frequency.

The theoretical capacity of the MIMO channel, using N_t transmitting antennas and N_r receiving antennas, increases linearly with $\min(N_t, N_r)$.

MIMO communication system has several advantages over other systems such as SIMO, SIMO and MISO, including:

- **Beamforming Gain:** This allows the signal to be directed towards a specific direction, which improves the quality and range of communication.
- **Spatial Diversity Gain:** By using multiple transmitting and receiving antennas, MIMO can mitigate the effects of channel fading and improve transmission reliability.

- **Spatial Multiplexing Gain:** Unlike SIMO and MISO systems, MIMO allows multiple independent data streams to be transmitted simultaneously on the same frequencies, thus increasing the overall throughput.

These first two advantages are also present in SIMO and MISO systems, however, spatial multiplexing gain is specific to MIMO, which gives it an additional advantage.

3.5 Optical MIMO (OMIMO)

It is common to use multiple luminaires to provide adequate illumination levels in various environments. In most cases, luminaires are equipped with multiple LEDs, which can be used as transmitters to facilitate the design and implementation of optical MIMO systems for VLC. With a similar objective as RF MIMO systems, optical MIMO uses multiple LEDs, to significantly improve the performance of VLC systems from a transmission perspective.

Consider a typical MIMO-OWC system equipped with N_t LED transmitters and N_r photodiode (PD) receivers. Let $s = [s_1, s_2, \dots, s_{N_t}]^T$ be the transmitted signal vector, H represents the MIMO channel matrix $N_r \times N_t$ and $n = [n_1, n_2, \dots, n_{N_r}]^T$ denotes the additive noise vector. The received signal vector $y = [y_1, y_2, \dots, y_{N_r}]^T$ can be given by:

$$y = Hs + n \quad (9)$$

Where, the channel matrix of the $N_r \times N_t$ MIMO-OWC system can be expressed as:

$$H_{N_r \times N_t} = \begin{bmatrix} h_{11} & \dots & h_{1N_t} \\ \vdots & \ddots & \vdots \\ h_{Nr1} & \dots & h_{NrN_t} \end{bmatrix} \quad (10)$$

in which, h_{rt} ($r = 1, 2, \dots, N_r$; $t = 1, 2, \dots, N_t$) is the channel gain between the r^{th} PD and the t^{th} LED.

There are three most common types of algorithms for VLC MIMO technology, which have been implemented by various researchers in the literature, namely, repetition coding (RC or spatial diversity 'SD'), spatial multiplexing (SMP), and spatial modulation (SM).

The most basic and easy to understand technique is SD, in which all transmitters transmit the same data signal simultaneously.

This algorithm performs well when designed for free-space optical systems due to its emission diversity. In addition, the signals transmitted by the different transmitters constructively add up at the receiver, increasing the overall system gain.

For SMP, all transmitters transmit different data signals simultaneously. Essentially, SMP leads to the creation of multiple parallel single-input single-output (SISO) data streams. This type of transmission poses a problem because it is imperative that the transmitter-receiver pair be precisely aligned with each other in order to mitigate inter-channel interference (ICI).

3.6 Digital Equalization Techniques

Digital equalization techniques are widely used in practice to attenuate the ISI arising from the LED frequency selective response, to help the VLC system operate beyond the 3 dB bandwidth of the LED. Digital equalization allows for hardware savings at the expense of computational complexity. For single-carrier modulation schemes, various types of time-domain equalizers can be used at the receiver. A feed forward equalizer (FFE) can be used with either zero-forcing (ZF) or minimum mean square error (MMSE) criteria.

3.6.1 Zero-Forcing (ZF) Equalizer

The Zero-Forcing (ZF) equalizer is a low-complexity linear equalizer named after the fact that it minimizes the ISI to zero, and provides a flat frequency response and linear phase due to the combination of channel and equalizer characteristics. However, this equalizer has drawbacks such as noise amplification, the need for accurate estimation of channel state information (CSI) for proper operation. The estimated signal vector, \hat{x} , using the ZF equalizer is chosen as the minimum error vector (least-squares solution) and is given by:

$$\hat{x} = \arg \min \|y - Hx\|^2 \quad (11)$$

$$\frac{d \|y - Hx\|^2}{dx} = \frac{d(y - Hx)^T (y - Hx)}{dx} \quad (12)$$

$$-2H^T \bar{y} + 2HH^T \hat{x} = 0 \quad (13)$$

$$\hat{x} = (H^T H)^{-1} H^T \bar{y} \quad (14)$$

$$\hat{x} = (H^H H)^{-1} H^H \bar{y} \quad (15)$$

Where, $(H^H H)^{-1} H^H$ is the pseudo-inverse of the channel matrix H . We should also note that the existence of an inverse cannot always be guaranteed, as is the case when the matrix does not have full rank and is therefore not invertible.

3.6.2 Minimum Mean Squared Error (MMSE) Equalizer

In this technique, the squared error of a random variable is first calculated and then its average is taken. The average value represents a very critical statistical difference. This MMSE equalizer is a linear equalizer that aims to attenuate the ISI and reduce the noise as well. The mathematical model of MMSE equalizer is given by:

$$\hat{x} = \arg \min E \|y - Hx\|^2 \quad (16)$$

$$= \arg \min E \{ \|C^{-T} \bar{y} - x\|^2 \} \quad (17)$$

The equalizer matrix is then as follows:

$$\bar{c} = P_d (P_d H H^T + \sigma_n^2 I)^{-1} H \quad (18)$$

Where P_d and σ_n^2 are the transmitted signal and noise powers at the receiver respectively.

Finally, the LMMSE equalizer for the MIMO system is given as follows:

$$\hat{x} = P_d (P_d H H^T + \sigma_n^2 I)^{-1} H \bar{y} \quad (19)$$

$$\hat{x} = P_d (P_d H H^H + \sigma_n^2 I)^{-1} H \bar{y} \quad (20)$$

The above equation can be rewritten as follows:

$$\hat{x} = \left(H H^H + \frac{1}{SNR} I \right)^{-1} H \bar{y} \quad (21)$$

Where, $SNR = \frac{P_d}{\sigma_n^2}$. Here, at high SNR, the MMSE equalizer approaches the ZF equalizer.

3.7 LED Models Configuration in VLC Indoor System

The proposed optical model schemes are modeled in a standard room with 5 m length, 5 m width and 3 m height, which corresponds to a dimension of $(5 \times 5 \times 3 \text{ m}^3)$. The optical emitters (16 LEDs) are distributed in three dimensions (3-D) on the ceiling, where the four centered LEDs are fixed to the ceiling and the others located under the ceiling at a distance D , this distance varies between 5 and 20 cm. knowing that D represents the value of the decline or the vertical distance from the ceiling.

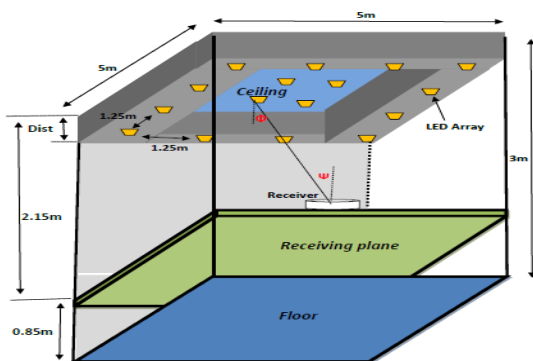


Figure 1: Arrangement of the First Model

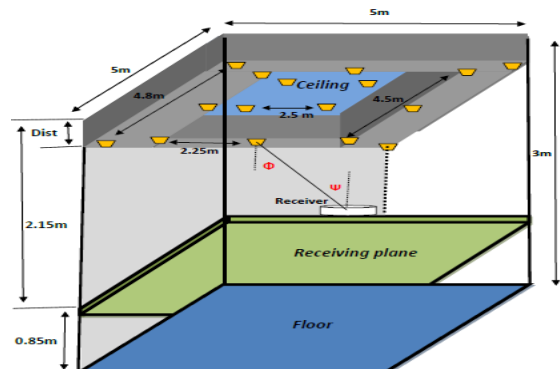


Figure 2: Arrangement of the Second Model

The receiver is assumed to be located above the floor on a desk. The height of the desk is 0.85 m, In addition, each LED matrix is filled with 900(30×30) LED chips, for a total number of 14400 LED chips. Typical room models are presented in Figure 1 and Figure 2, while the top views of both models are presented in Figure 3(a) and Figure 3(b) respectively.

The top view of each proposed model is similar to a scheme already presented in the literature, the first proposed model is similar to Khadr's scheme [20], while the second proposed model is similar to Mahfouz's model [21].

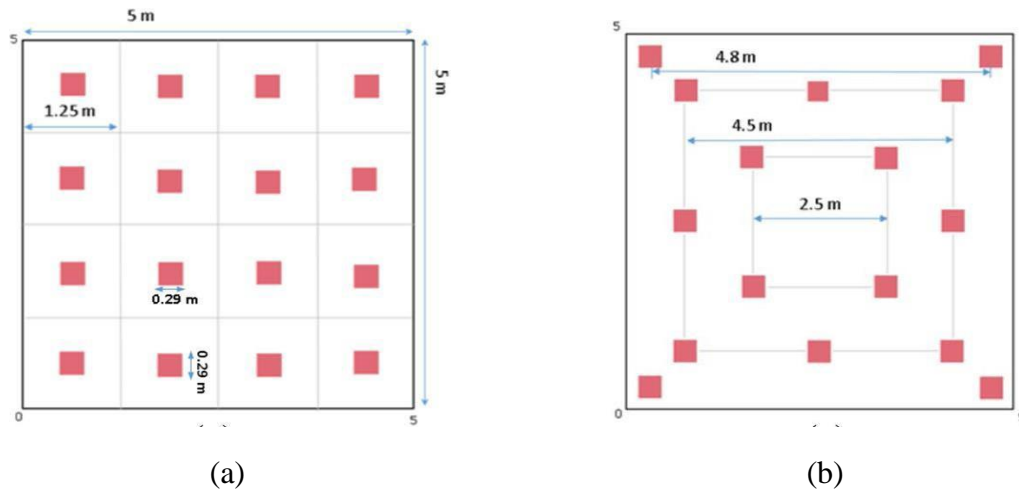


Figure 3: Top View of the Proposed Models: (a) First Model, and (b) Second Model

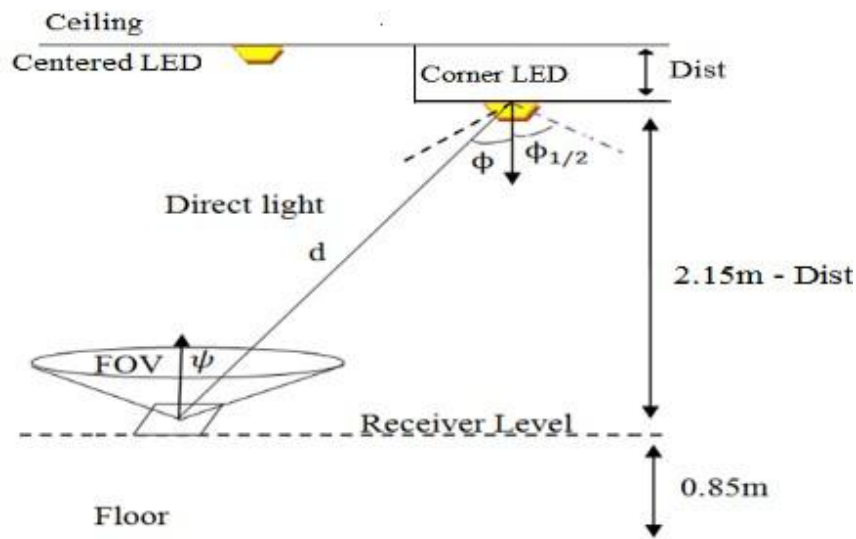


Figure 4: The Geometric Configuration of the System

Then, the proposed arrangements are compared to the previously presented models [20] [21] which have zero vertical distance from the ceiling ($D=0$). The geometry of the proposed arrangement is illustrated in Figure 4, where only the Line-Of-Sight (LOS) has been considered. The different parameters used in the simulation are presented in Table 1.

3.7.1 Modeling of the Proposed VLC Systems

The light emission occurs in all directions around the entire surface of the LEDs, which is called Lambertian emission. The optical power intensity is the power radiated through a unit solid angle on a unit surface. The maximum intensity I_0 occurs in the direction perpendicular to the LED surface. The radiation intensity $I(\phi)$ of the optical source depends on the irradiation angle ϕ and is as follows:

$$I(\phi) = I(0) \cos^m(\phi) \quad (22)$$

Where ϕ is the illumination angle with respect to the axis normal to the transmitter surface. $I(0)$ is the central luminous intensity, and the Lambertian order m is given by:

$$m = -\frac{\ln 2}{\ln(\cos \phi_{1/2})} \quad (23)$$

3.7.2 Transmission Channel

In our study, we limit the propagation of light beams only in the line-of-sight (LOS) channel, where the DC gain of the LOS channel is modeled by:

$$H_{LOS} = \begin{cases} \frac{A_r(m+1) \cos^m(\phi) T_s(\Psi) g(\Psi) \cos(\Psi)}{2\pi D^2} & 0 \leq \Psi \leq \Psi_c \\ 0 & otherwise \end{cases} \quad (24)$$

At the receiving end, optical filters and concentrators are respectively used to attenuate ambient light in the optical receivers and to increase the effective light collecting area.

4. Results and Discussion

Table 1: Simulation Parameters

	Parameters	Values
Chamber	Size	5×5×3 m ³
Source	Total number of μ LEDs	14.400 (30*30*16)
	Transmitted power of μ LEDs	20mW
	Half-power angle	70°
	Receiver plane above ground	0.85 m
	Active area	1 cm ²
	Half-angle FOV	70°
	Lens refractive index	1.5

Receiver	Optical filter gain	1
	Photodiode responsivity (R)	0.54
	Bandwidth factor (I_2)	0.562
	Bit rate (B)	30 Mb/s
	Absolute temperature (T_k)	298 K
	Fixed capacitance per unit area (η)	112pF/cm ²
	FET channel noise figure (Γ)	1.5
	FET transconductance (g_m)	30 mS
	Bandwidth factor (I_3)	0.0868

This chapter presents the simulation results based on the methodology outlined in Section 3, focusing on evaluating the performance of the VLC system under different configurations and scenarios. The results cover key performance metrics such as illuminance, received power, signal-to-noise ratio (SNR), and throughput. The findings confirm the effectiveness of the proposed 3D LED arrangement and various MIMO techniques in improving the system's efficiency. A comparative analysis with existing systems further demonstrates the advantages of the proposed models.

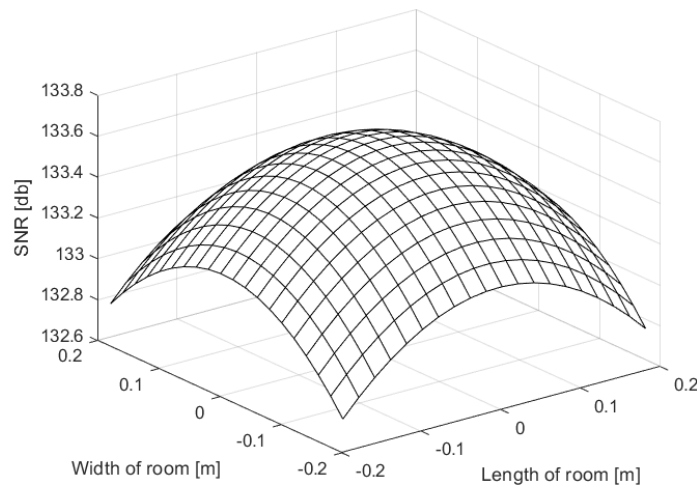


Figure 5: 3D Plot for Room SNR Distribution with Lens

Figure 5 presents a 3D visualization of the Signal-to-Noise Ratio (SNR) distribution across the room when a lens is used. The plot highlights how the SNR varies across different spatial locations in the room. With the lens, the SNR improves in areas close to the receiver, due to the enhanced focus and directionality of the transmitted light. This improved SNR ensures optimal communication quality in focused regions of the room.

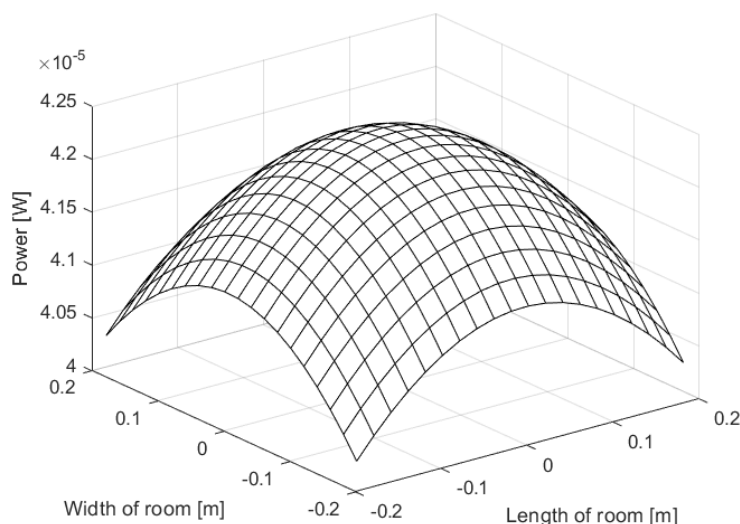


Figure 6: 3D Plot for Received Power Distribution

Figure 6 shows a 3D plot depicting the received power distribution throughout the room. Received power is crucial for determining the strength of the signal at the receiver. The plot visualizes areas with higher signal strength and regions where the signal is weaker, providing insight into the overall performance and coverage of the system.

Figure 7 shows the received power distribution but without the use of a lens. The absence of the lens results in a less focused transmission, leading to a more widespread and weaker signal coverage across the room. This figure highlights how the received power diminishes, especially in areas further from the light source.

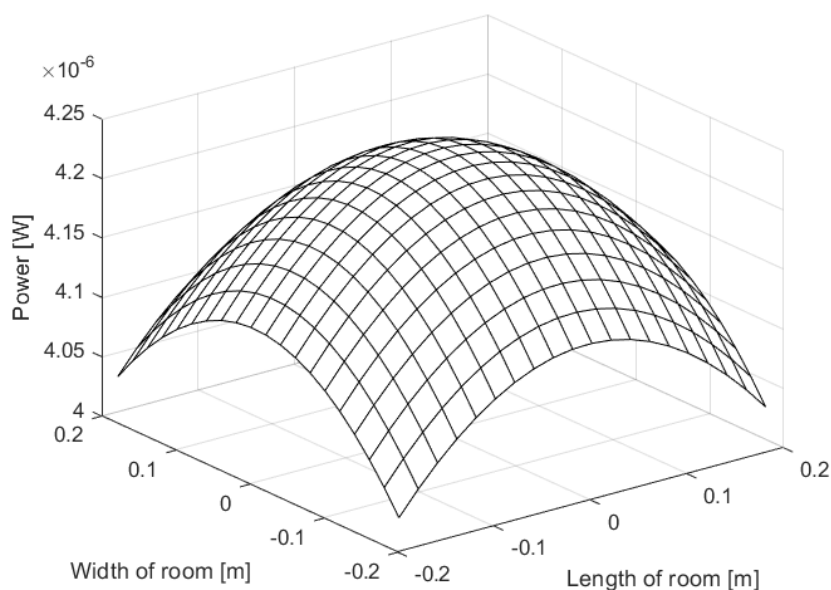


Figure 7: 3D Plot for Received Power Distribution without Lens

Figure 8 quantifies the total received power across the room in watts. This figure gives an overall measure of the signal strength received by the system, offering a comprehensive view of the signal's strength across the entire space. The total received power is an important metric for assessing the reliability and quality of the communication link, determining if the received signal is sufficient for effective data transmission.

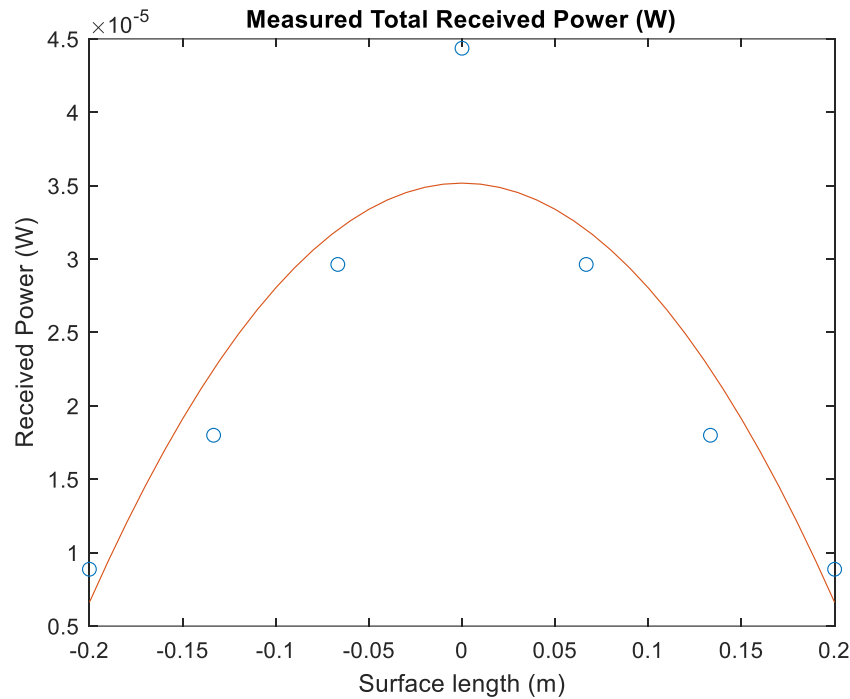


Figure 8: Measured Total Received Power (W)

Figure 9 displays the output signal in the frequency domain. This graph shows the distribution of signal power across different frequencies, which is crucial for understanding the bandwidth utilization of the VLC system. Frequency analysis helps in identifying potential frequency interference that may negatively impact the system's performance.

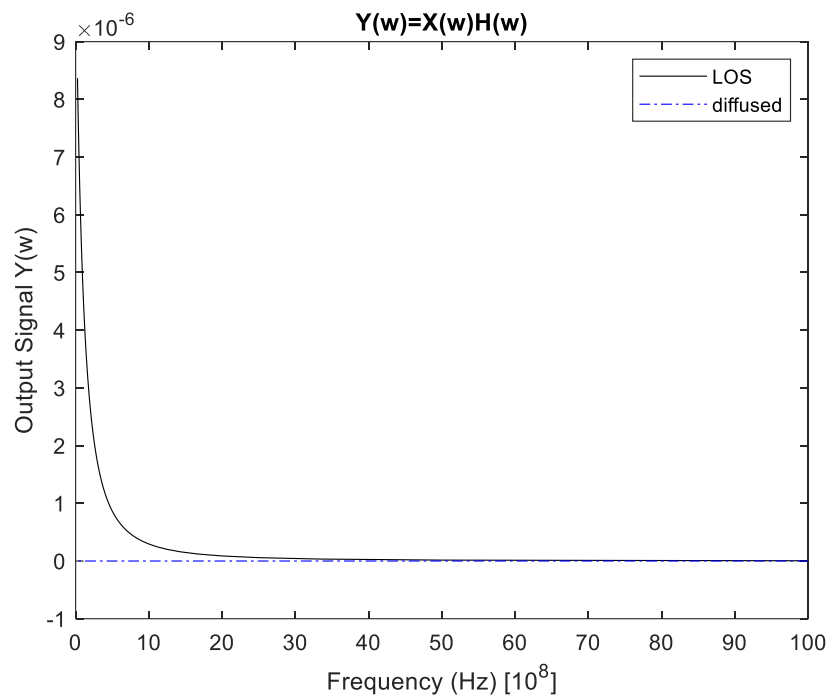


Figure 9: Graphical representation of output signal $y(t)$ vs. frequency

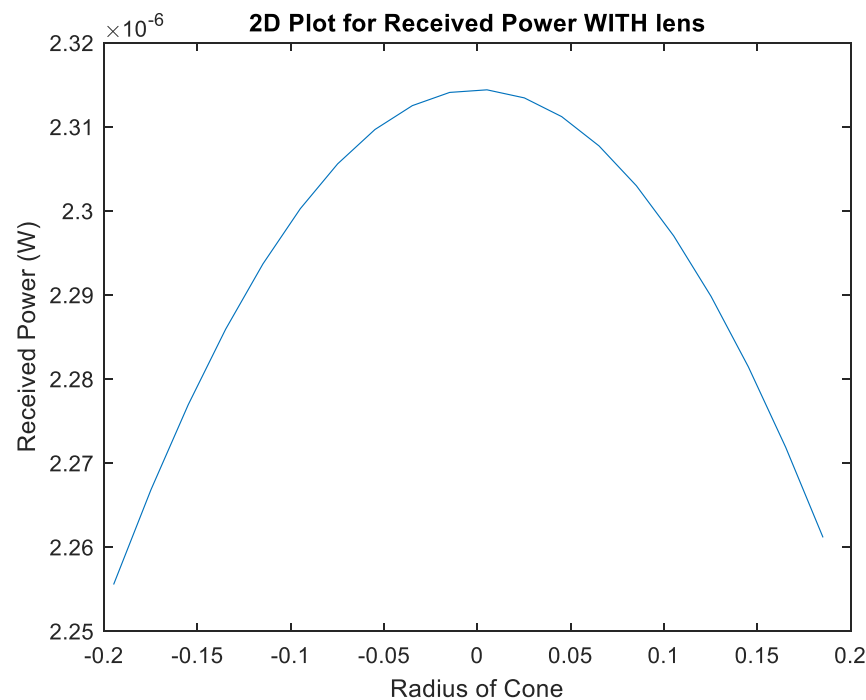


Figure 10: 2D plot for Received Power with Lens

Figure 10 presents a 2D plot of received power across the room with the use of a lens. The plot highlights how the lens improves the received power in certain regions of the room by concentrating the signal strength in specific areas. This visual representation makes it easier to evaluate how the lens affects the distribution of received power within the room.

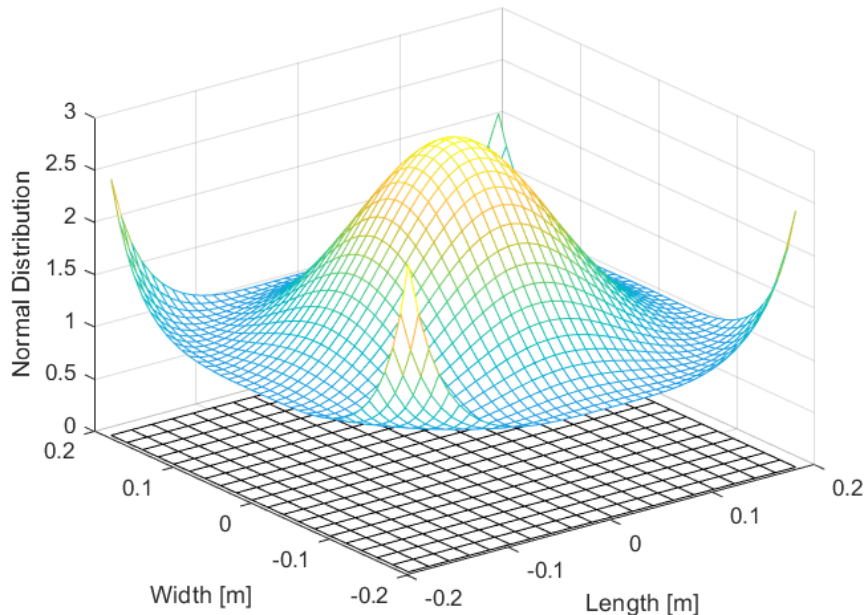


Figure 11: 3D Plot for Received Power Distribution

Figure 11 displays the received power distribution in the room without the lens or any other modifications. This figure helps establish a baseline for evaluating the system's performance under normal conditions. It allows comparisons with the results from other configurations, such as those with lenses, to assess the effectiveness of various system setups.

Figure 12 demonstrates the performance of a Single Input Single Output (SISO) channel in a VLC system. This figure shows how the signal is transmitted and received using a single antenna at both the transmitter and receiver. It serves as a basic reference for understanding SISO performance and comparing it to more complex systems like MIMO.

5. Conclusion

This paper proposed a novel indoor Visible Light Communication (VLC) system utilizing a LED arrangement coupled with MIMO techniques to enhance data throughput and communication reliability. The results from the simulations demonstrate that the integration of

MIMO systems significantly improves the performance of VLC systems in indoor environments, as evidenced by enhanced signal-to-noise ratios, received power, and throughput. The comparison with traditional SISO systems further highlights the advantages of the proposed setup in reducing interference and increasing data rates. The use of optical lenses was found to enhance the SNR in focused areas, offering potential for practical deployment in environments requiring high communication efficiency. Additionally, the findings suggest that the proposed VLC system can provide a scalable and cost-effective solution, using existing lighting infrastructure to support the growing demand for high-speed wireless communication. Future work will explore further optimizations, including non-line-of-sight (NLoS) scenarios and the integration of advanced modulation schemes for improving system capacity in dynamic indoor environments.

REFERENCES

- [1] Burchardt, H., Serafimovski, N., Tsonev, D., Videv, S., & Haas, H. (2014). VLC: Beyond point-to-point communication. *IEEE Communications Magazine*, 52(7), 98–105.
- [2] Chen, X., Ng, D. W. K., Yu, W., Larsson, E. G., Al-Dhahir, N., & Schober, R. (2021). Massive access for 5G and beyond. *IEEE Journal on Selected Areas in Communications*, 39(3), 615-637.
- [3] Cisco. (2020). Cisco Annual Internet Report (2018–2023) White Paper. Cisco. San Jose, CA, USA.
- [4] Fath, T., & Haas, H. (2013). Performance comparison of MIMO techniques for optical wireless communications in indoor environments. *IEEE Transactions on Communications*, 61(2), 733–742.
- [5] Gui, G., Liu, M., Tang, F., Kato, N., & Adachi, F. (2020). 6G: Opening new horizons for integration of comfort, security, and intelligence. *IEEE Wireless Communications*, 27(5), 126-132.
- [6] International Energy Agency. (2020). Lighting sales by type in the Sustainable Development Scenario, 2010–2030. Retrieved from <https://www.iea.org/data-and-statistics/charts/lighting-sales-by-type-in-the-sustainable-development-scenario-2010-2030>

- [7] Jovicic, A., Li, J., & Richardson, T. (2013). Visible light communication: Opportunities, challenges and the path to market. *IEEE Communications Magazine*, 51(12), 26-32.
- [8] Karunatilaka, D., Zafar, F., Kalavally, V., & Parthiban, R. (2015). LED-based indoor visible light communications: State of the art. *IEEE Communications Surveys & Tutorials*, 17(3), 1649-1678.
- [9] Mahmoud, M., Boghdady, A. I., El-Fikky, A. E. R. A., & Aly, M. H. (2021). Statistical studies using goodness-of-fit techniques with dynamic underwater visible light communication channel modeling. *IEEE Access*, 9, 57716-57725.
- [10] El-Fikky, A. E. R. A., Eldin, M. E., Fayed, H. A., El Aziz, A. A., Shalaby, H. M., & Aly, M. H. (2019). NLoS underwater VLC system performance: static and dynamic channel modeling. *Applied optics*, 58(30), 8272-8281.
- [11] Anous, N., Abdallah, M., Uysal, M., & Qaraqe, K. (2018). Performance evaluation of LOS and NLOS vertical inhomogeneous links in underwater visible light communications. *IEEE Access*, 6, 22408-22420.
- [12] Nasser, A. G., & Ali, M. A. A. (2024). Performance of LED for line-of-sight (LoS) underwater wireless optical communication system. *Journal of Optical Communications*, 44(s1), s1355-s1363.
- [13] Chi, N., & Shi, M. (2019, September). Enabling technologies for high-speed LED based underwater visible light communications. In *2019 IEEE International Conference on Signal Processing, Communications and Computing (ICSPCC)* (pp. 1-4). IEEE.
- [14] Hamagami, R., Ebihara, T., Wakatsuki, N., & Mizutani, K. (2021). Optimal modulation technique for underwater visible light communication using rolling-shutter sensor. *IEEE Access*, 9, 146422-146436.
- [15] Christopoulou, C., Sandalidis, H. G., & Vaiopoulos, N. (2020). Performance of an underwater optical wireless link with a randomly placed or moving receiver. *IEEE Journal of Oceanic Engineering*, 46(3), 1068-1079.
- [16] Elamassie, M. and Uysal, M., 2020. Vertical underwater visible light communication links: Channel modeling and performance analysis. *IEEE Transactions on Wireless Communications*, 19(10), pp.6948-6959.

- [17] Babalola, O. P., & Balyan, V. (2020). Efficient channel coding for dimmable visible light communications system. *IEEE Access*, 8, 215100-215106.
- [18] Matheus, L. E. M., Vieira, A. B., Vieira, L. F. M., Vieira, M. A. M., & Gnawali, O. (2019). Visible light communication: Concepts, applications and challenges. *IEEE Communications Surveys & Tutorials*, 21(4), 3204-3237.
- [19] Miramirkhani, F., Karbalayghareh, M., Zeydan, E., & Mitra, R. (2022). Enabling 5G indoor services for residential environment using VLC technology. *Physical Communication*, 53, 101679.
- [20] Khadr, M. H., Fayed, H. A., Abd El Aziz, A., & Aly, M. H. (2016, July). Bandwidth extension of an enhanced SNR with a higher light uniformity of a phosphorescent white LED based visible light communication system. In 2016 10th international symposium on communication systems, networks and digital signal processing (CSNDSP) (pp. 1-6). IEEE.
- [21] Mahfouz, N. E., Fayed, H. A., Abd El Aziz, A., & Aly, M. H. (2018). Improved light uniformity and SNR employing new LED distribution pattern for indoor applications in VLC system. *Optical and Quantum Electronics*, 50, 1-18.

Citation: Faheem Mollick, Shanti Rathore, Kiran Tigga. A Novel Indoor Visible Light Communication System Using MIMO Techniques and LED Placement for Enhanced Signal Quality. *International Journal of Electronics and Communication Engineering and Technology (IJCET)*, 16(1), 2025, pp. 1-20.

Article Link:

https://iaeme.com/MasterAdmin/Journal_uploads/IJCET/VOLUME_16_ISSUE_1/IJCET_16_01_001.pdf


Abstract Link:

https://iaeme.com/Home/article_id/IJCET_16_01_001

Copyright: © 2025 Authors. This is an open-access article distributed under the terms of the Creative Commons Attribution License, which permits unrestricted use, distribution, and reproduction in any medium, provided the original author and source are credited.

This work is licensed under a **Creative Commons Attribution 4.0 International License (CC BY 4.0)**.



 editor@iaeme.com